# A Resistor-Based Temperature Sensor with a 0.13pJ·K2 Resolution FOM

Pan, Sining; Luo, Yanquan; Heidary Shalmany, Saleh; Makinwa, Kofi A.A.

**DOI**
10.1109/ISSCC.2017.7870309

**Publication date**
2017

**Document Version**
Accepted author manuscript

**Published in**
2017 IEEE International Solid-State Circuits Conference, ISSCC 2017

## 9.1 A Resistor-Based Temperature Sensor with a 0.13pJ·K² Resolution FOM

Sining Pan[1], Yanquan Luo[1,2], Saleh Heidary Shalmany[1,3], Kofi A.A. Makinwa[1]

[1]Delft University of Technology, Delft, The Netherlands
[2]Ulm University, Ulm, Germany
[3]Broadcom, Bunnik, The Netherlands

Temperature sensors are often used for the temperature compensation of frequency references [1-5]. High resolution and energy efficiency are then critical requirements, the former to minimize jitter and the latter to minimize power dissipation in a given conversion time. A MEMS-resonator-based sensor meets both criteria [1], but requires two resonators. In principle, resistor-based sensors also meet these criteria, and are CMOS compatible, but previous designs have been limited by the power dissipation [2-4] or 1/*f* noise [6] of their readout electronics. This paper describes a CMOS temperature sensor that digitizes the temperature-dependent phase shift of an RC filter. It achieves 410μ$K_{rms}$ resolution in a 5ms conversion time, while consuming only 160μW. This corresponds to a resolution FOM of 0.13pJ·K², a 5× improvement on previous CMOS sensors [6].

As shown in Fig. 9.1.1, the sensor is based on a Wien bridge (an RC bandpass filter), which is driven at its center frequency $f_{drive} = 1/(2\pi RC)$ by a rail-to-rail square-wave derived from a frequency reference [2,3]. The bridge's temperature-dependent phase-shift is then digitized by a phase-domain ADC. Since on-chip (MIM) capacitors are quite stable, this phase-shift mainly reflects the resistor's temperature dependency. Although the use of AC drive avoids the 1/*f* noise of the readout electronics, the bridge resistors themselves exhibit 1/*f* noise (resistance fluctuations). To investigate the relationship between 1/*f* noise and resistivity, bridges from two types of resistors were built: silicided p-poly (0.36%/°C) and non-silicided n-poly (-0.17%/°C). Poly resistors were chosen for their low voltage dependence compared to diffusion resistors. With the chosen values ($R$=32kΩ, $C$=10pF, $f_{drive}$=500kHz), the thermal noise of the p-poly bridge alone translates into a room temperature (RT) resolution of 280μK in a conversion time $T_{conv}$ of 5ms. Each bridge is driven by a pair of large inverters, whose output impedance (<20Ω) and phase delay (<4m°) are negligible compared to those of the bridge.

As shown in Fig. 9.1.2, the temperature-dependent phase shift of each bridge is digitized by a phase-domain ΔΣmodulator (PDΔΣM). Compared to [2,3], the use of an active 1st integrator lowers the input impedance, while the use of a 2nd-order loop enables higher resolution in a given conversion time. Stabilization via a feedforward coefficient, implemented by $R_{ff}$ in Fig. 9.1.2, requires only one phase-domain DAC and reduces the modulator's internal swing. The Wien bridge's output currents can then be accurately sensed by connecting its output resistors to the 1st integrator's virtual ground. The phase shift of these currents is then detected by a chopper demodulator, which is driven by a clock with a bitstream-controlled phase shift, and then integrated. The chopper also suppresses the 1st integrator's offset and 1/*f* noise. On-chip logic is used to derive $f_{drive}$ and two phase references ($\phi_1$ = 67.5° and $\phi_2$ = 112.5°) from an 8MHz clock.

The opamp in the 1st integrator consists of a telescopic OTA and two PMOS source followers. Compared to an OTA, the use of an opamp significantly reduces the integrator's input impedance and input swing. This, in turn, improves its linearity and minimizes the modulation of 1/*f* noise to odd harmonics of $f_{drive}$, which the chopper demodulator would then translate into residual phase offset and 1/*f* noise. The OTA is based on a PMOS input pair, whose tail current (16μA at RT) was optimized for low noise and power consumption, while the source followers' bias current (20μA each at RT) was chosen to handle the bridge's peak output current (16μA at -40°C for the p-poly bridge). The 2nd integrator consists of a telescopic OTA based on a source-degenerated NMOS input pair, which draws only 3.6μA.

Two sensors, based on the p-poly and n-poly bridges, were fabricated side-by-side in a TSMC 180nm CMOS process (Fig. 9.1.7). They share the same constant-gm biasing and clock generation circuits. Each sensor consumes 87μA from a 1.8V supply, and occupies 0.72mm², about 40% of which is occupied by the 1st integrator's capacitors (2 × 180pF).

FFTs of the bit-stream outputs of both sensors are shown in Fig. 9.1.3. It can be seen that the sensor's noise floor is dominated by the bridges' thermal noise. For this measurement, the sensors are driven by a low-jitter (1p$s_{rms}$) frequency reference, which contributes less than 0.5% of the total noise power. The sensors were mounted in good thermal contact with a large aluminum block to minimize the effect of ambient temperature drift. Figure 9.1.3 (bottom) shows the resolution vs. conversion time plot of both sensors, obtained after sinc² decimation of their bitstream outputs. In a 5ms conversion time, the n-poly resistor achieves 880μ$K_{rms}$ resolution, while the p-poly achieves 410μ$K_{rms}$ resolution, due to its higher sensitivity. The n-poly resistor exhibits a 1/*f* corner of about 10Hz, while that of the p-poly sensor is below 0.1Hz, and in fact, is obscured by ambient temperature drift. These results demonstrate the effectiveness of the 1/*f* noise-cancellation techniques.

Twenty samples from one wafer were characterized in ceramic DIL packages from –45 to 85°C. Figure 9.1.4 shows their output phase shift over temperature. At RT, supply sensitivities of -0.17°C/V (p-poly bridge) and 0.34°C/V (n-poly bridge) were observed for supply voltages ranging from 1.6 to 2V. After correcting the modulator's inherent cosine non-linearity [7], the n-poly bridge achieves a 3σ inaccuracy of 0.25°C from -45 to 85°C (step of 10°C), after a 1st-order fit followed by a fixed correction of the resistor's systematic non-linearity [3]. Over the same range, the p-poly bridge is more reproducible, achieving a 3σ inaccuracy of 0.07°C. Moreover, the coefficients of its 1st-order fit turn out to be strongly correlated, in a manner which agrees well with simulations (Fig. 9.1.5). By exploiting this, a 3σ inaccuracy of 0.2°C was achieved with a one-point trim, which is similar to the inaccuracy of BJT-based sensors [8].

In Fig. 9.1.6, the performance of the p-poly bridge is summarized and compared to other high-resolution temperature sensors. Based on Fig. 9.1.6, it achieves the lowest resolution FOM for a CMOS temperature sensor, and its resolution (in a given conversion time) is only matched by [4], which requires much more energy. These results demonstrate that silicided poly resistors can be used to realize the high resolution and energy-efficient sensors required for the temperature compensation of precision frequency references.

*Acknowledgments:*
We thank Zu-yao Chang and Lukasz Pakula for their assistance in building the measurement setup.

*References:*
[1] M. H. Roshan, et al., "Dual-MEMS-Resonator Temperature-to-Digital Converter with 40μK Resolution and FOM of 0.12pJK²," *ISSCC*, pp. 200-201, 2016.
[2] P. Park, et al., "A Resistor-Based Temperature Sensor for a Real Time Clock with ±2ppm Frequency Stability," *IEEE JSSC*, vol. 50, no. 7, pp. 1571-1580, July 2015.
[3] M. Shahmohammadi, et al., "A resistor-based temperature sensor for MEMS frequency references," *ESSCIRC*, pp. 225-228, 2013.
[4] M. Perrott, et al., "A Temperature-to-Digital Converter for a MEMS-based Programmable Oscillator with < ±0.5-ppm Frequency Stability and < 1-ps Integrated Jitter," *IEEE JSSC*, vol. 48, no. 1, pp. 276-291, Jan. 2013.
[5] S. Zaliasl, et al., "A Micro-Power Temperature-to-Digital Converter for Use in a MEMS-Based 32 kHz Oscillator," *Efficient Sensor Interfaces, Advanced Amplifiers and Low Power RF Systems*, pp. 65-79, 2016.
[6] C. Weng, et al., "A CMOS Thermistor-Embedded Continuous-Time Delta-Sigma Temperature Sensor With a Resolution FoM of 0.65 pJ °C²," *IEEE JSSC*, vol. 50, no. 11, pp. 2491-2500, Jan. 2015.
[7] S.M. Kashmiri, et al., "A Temperature-to-Digital Converter Based on an Optimized Electrothermal Filter," *IEEE JSSC*, vol. 44, no. 7, pp. 2026-2035, July 2009.
[8] A. Heidary, et al., "A BJT-Based CMOS Temperature Sensor with a 3.6pJ·K²-resolution FoM," *ISSCC*, pp. 224-225, 2014.

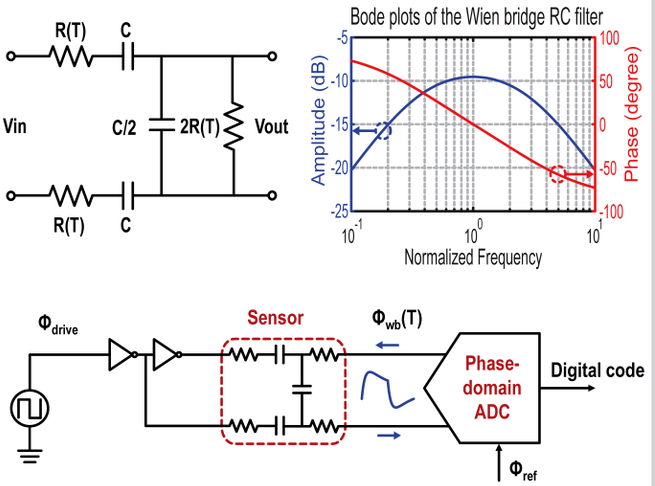


**Figure 9.1.1: Wien bridge sensor structure (top left), Bode plot of the sensor (top right) and system block diagram (bottom).**

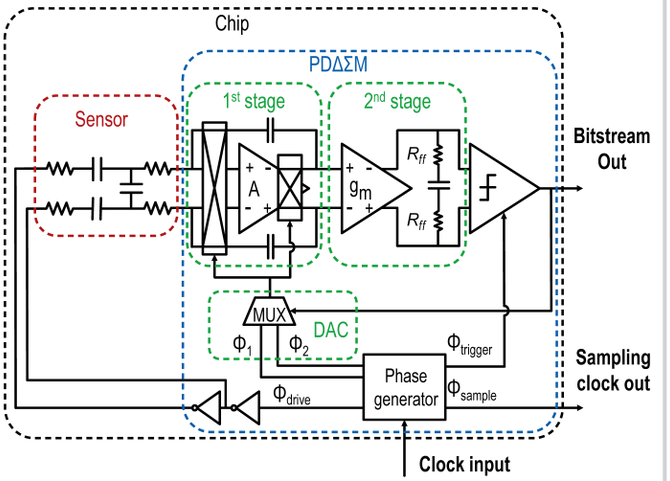


**Figure 9.1.2: Full system block diagram.**

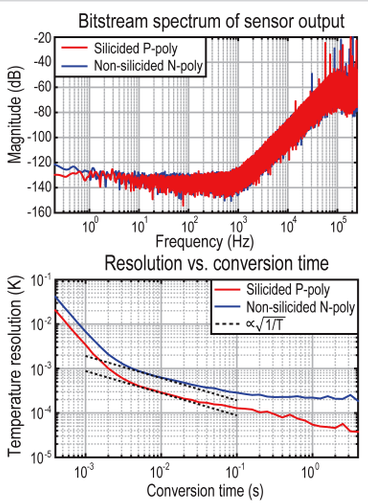


**Figure 9.1.3: PSD of the sensor's bitstream obtained from 2,500,000 samples with a Kaiser window (top) and its resolution vs. conversion time plot (bottom).**

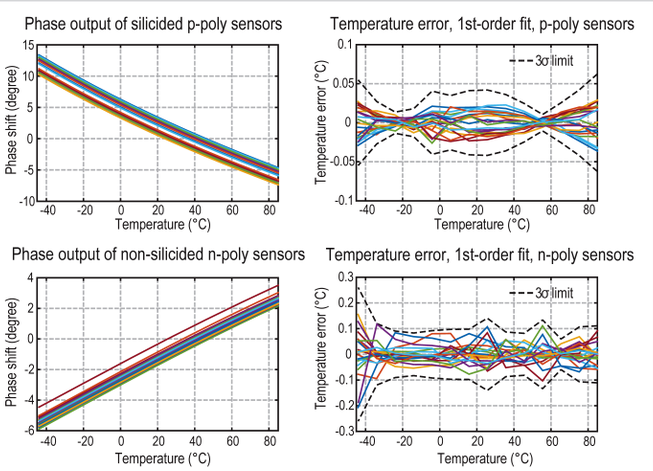


**Figure 9.1.4: Sensors' output phase (left) and temperature error after 1st-order polynomial fitting and systematic error removal (right) for silicided p-poly (top) and non-silicided n-poly (bottom) sensors.**

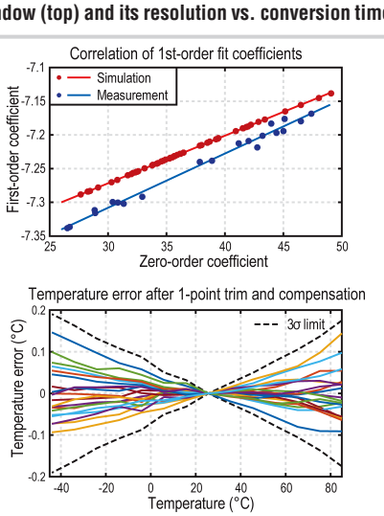


**Figure 9.1.5: Correlation of the coefficients in the 1st-order fit of the silicided p-poly sensor (top) and the remaining temperature error after a 1-point trim exploiting this correlation (bottom).**

| | **This work** | [1] | [2] | [4] | [6] | [8] |
|---|---|---|---|---|---|---|
| Sensor type | **Resistor** | Dual-MEMS Resonator | Resistor | Resistor | Resistor | BJT |
| CMOS Technology | **0.18µm** | 0.18µm | 0.18µm | 0.18µm | 0.18µm | 0.7µm |
| Area [mm²] | **0.72** | 0.54 | 0.09 | 0.18 | 0.43 | 1.5 |
| Power consumption [mW] | **0.16** | 19 | 0.031 | 13 | 0.065 | 0.16 |
| Temperature range | **-40°C to 85°C** | -40°C to 85°C | -40°C to 85°C | -40°C to 85°C | -40°C to 125°C | -40°C to 125°C |
| Conversion time [ms] | **5** | 3.85 | 32 | 100 | 0.1 | 2.2 |
| Resolution [mK] | **0.41** | 0.04 | 2.8 | 0.1 | 10 | 3 |
| Resolution FoM [pJ·K²]* | **0.13** | 0.12** | 8 | 13 | 0.65 | 3.6 |

* Resolution FoM = (Energy / Conversion) x (Resolution)²
** Not fully CMOS compatible

**Figure 9.1.6: Performance summary and comparison with previous works.**

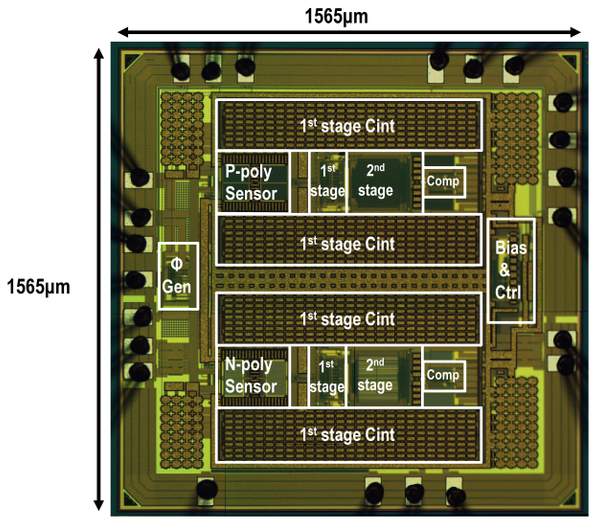


**Figure 9.1.7: Die micrograph of the fabricated temperature sensor.**